

HUMAN SHAPE FEATURE DETECTION SYSTEM BASED ON 3D LASER SCANNING

Chunyan LIU¹, Xiayan SI^{2*}, Baodong WANG³, Yan DAI⁴, Yingji WANG⁵,
Jianwei WANG⁶, Chengyu YIN⁷, Liangyu CHEN⁸

In order to realize the intelligent adjustment of the seat, a body shape feature detection system was designed based on 3D laser scanning. The system was composed of a three-dimensional laser scanning module, data processing module and control feedback module. The principle of laser binocular vision was used to the system for obtaining laser scanning information in different positions. Feature points in different positions were extracted to calculate two angle values representing comfort. According to the mathematical model of human body shape characteristic structure and the position and posture of seat, the seat was automatically adjusted by control parameters. In simulation analysis, the sampling effect of the test curve at different frequencies was compared. The error between the control chord height method and the known curve function was small. In the experiment, the average positioning accuracy of the system was about 0.035 mm, which can effectively ensure the coordinate measurement accuracy of feature positions. At the same time, in the curve reconstruction experiment, the accurate parameters of the scanning path for the human body shape were obtained, and the automatic data acquisition of the TCP robot was realized. It was verified that the algorithm can automatically adjust by the actual position of the tester, to achieve comfort optimization.

Keywords: laser scanning; shape feature of human body; point cloud data analysis; binocular vision

¹ A. Prof., School of Electrical Engineering, Changchun College of Electronic Technology, e-mail: 349328793@qq.com

² A. Prof., School of Electrical Engineering, Changchun College of Electronic Technology, e-mail: sixiayan@qq.com (Corresponding Author)

³ Senior Engineer, Product Innovation Department, Changchun Fusheng automobile technology R & D Co., Ltd, e-mail: bwang04@fawsn-autoparts.com

⁴ Prof., School of Electrical Engineering, Changchun College of Electronic Technology, e-mail: 635999914@qq.com

⁵ Prof., School of Electrical Engineering, Changchun College of Electronic Technology, e-mail: 2424985764@qq.com

⁶ Assistant Engineer, Product Innovation Department, Changchun Fusheng automobile technology R & D Co., Ltd, e-mail: Wjw6174@163.com

⁷ Student, School of Electronic Engineering, Changchun College of Electronic Technology, e-mail: 2084449124@qq.com

⁸ Student, School of Electronic Engineering, Changchun College of Electronic Technology, e-mail: 2542774185@qq.com

1 Introduction

In order to obtain the characteristic size of the human body, the traditional method mainly relied on equipment such as a soft ruler, an altimeter, and a goniometer for the human body [1]. There was random errors by the measurement experience of the inspectors, and it reduced test accuracy [2]. With the development of computer vision technology and 3D laser scanning technology, there were many methods to obtain 3D data of the human body. The feature size of human body can be obtained by measuring 3D point cloud data [3]. Compared with the traditional measurement methods, it was poor efficiency and low degree of automation. There weren't the shortcomings of traditional methods for 3D measurement technology, and its characteristics were high speed, high efficiency and high automation [4]. 3D point cloud data processing is widely used, and it's of great significance. For the 3D data model containing human features, whether it is a complete digital model or a depth image model, it can provide data support for automatic control technology.

There were many methods for 3D human reconstruction, which were mainly used in the test field. Human 3D reconstruction used single or multi-frame data by a 3D scanner to reconstruct a static 3D human body model [5]. Image-based reconstruction method refers to using single or multiple images to accurately reconstruct a 3D human body model. Chen J Y et al. [6] constructed a convolutional neural network to reconstruct a human body model by binary images of human contours. The human body model was reconstructed by the mapping relationship with the point cloud data of the 3D human body model. This method could quickly reconstruct the human body model, but it was hard to modify the details of the reconstructed human body model. The human body reconstruction method based on specific software did not need to take up a lot of data resources. For example, Wu X C [7] proposed to complete the virtual human model based on Unity-3D, which could control the posture of the virtual human. But it had a poor description of human body dynamics and required sufficient knowledge to realize. Wang et al. [8] developed a 3D modeling system. Based on the standard model, the parameters were modified to generate a personalized 3D human model. Its speed of modeling and accuracy were high, but it was difficult to determine the main characteristic parameters of the human body. Liu Y M et al. [9] used the Vitus Smart 3D body scanner to build a series of virtual avatars for children. This method completed the transformation from 2D fitting to 3D fitting, but the scanner was bulky and expensive. It was high requirements for environment and machine performance.

Laser 3D scanning technology [10] had been applied to the field of vehicle seat adjustment. The real-time automatic adjustment of the car seat can be realized

by quickly obtaining the driver's feature performances. A body shape feature detection system was proposed based on laser 3D scanning.

2 3D Laser Scanning Principle

The measuring equipment consisted of camera A, camera B and projection lens [11]. The coordinate system of camera A was $X_L Y_L Z_L$, and the coordinate system of camera B was $X_R Y_R Z_R$. The corresponding imaging plane coordinate systems were $x_l y_l$ and $x_r y_r$, respectively. Camera A was used as the coordinate of the binocular vision system, which was $X_s Y_s Z_s$. The mark point was a point in space, and the point was in the common field of the two cameras. Its coordinates in the system $X_s Y_s Z_s$ were set to $(X_p Y_p Z_p)$, and point P was also in the grating fringe area by the projection lens. The principle of the test system was shown in Figure 1.

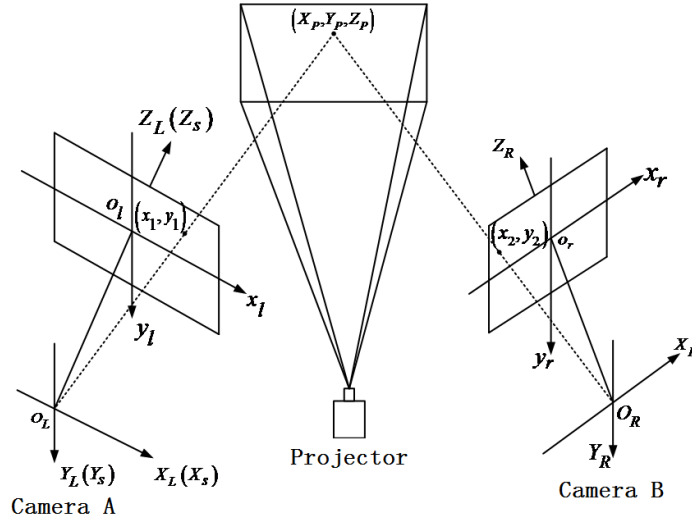


Fig.1 Principle model of laser scanning system

The camera imaging model can obtain the relationship matrix between the two cameras as [12]:

$$\begin{bmatrix} X_l \\ Y_l \\ Z_l \\ 1 \end{bmatrix} = \begin{bmatrix} r_{11} & r_{12} & r_{13} & t_1 \\ r_{21} & r_{22} & r_{23} & t_2 \\ r_{31} & r_{32} & r_{33} & t_3 \\ 0 & 0 & 0 & 1 \end{bmatrix} \begin{bmatrix} X_r \\ Y_r \\ Z_r \\ 1 \end{bmatrix} \quad (1)$$

Among them, R represents the rotation matrix of the two cameras, and T represents the translation matrix of the two cameras.

$$R = \begin{bmatrix} r_{11} & r_{12} & r_{13} \\ r_{21} & r_{22} & r_{23} \\ r_{31} & r_{32} & r_{33} \end{bmatrix}, \quad T = \begin{bmatrix} t_1 \\ t_2 \\ t_3 \end{bmatrix} \quad (2)$$

According to the coordinate transformation principle of the linear camera [13], the coordinate of the point in the world coordinate $X_sY_sZ_s$ is (X_p, Y_p, Z_p) , and the transformation relationship between P and the corresponding image points in the two cameras is

$$\rho_1 \begin{bmatrix} x_1 \\ y_1 \\ 1 \end{bmatrix} = \begin{bmatrix} c_1 & 0 & 0 & 0 \\ 0 & c_2 & 0 & 0 \\ 0 & 0 & 1 & 0 \end{bmatrix} \begin{bmatrix} X_p \\ Y_p \\ Z_p \\ 1 \end{bmatrix}, \quad \rho_2 \begin{bmatrix} x_2 \\ y_2 \\ 1 \end{bmatrix} = \begin{bmatrix} c_2 r_{11} & c_2 r_{12} & c_2 r_{13} & c_2 t_1 \\ c_2 r_{21} & c_2 r_{22} & c_2 r_{23} & c_2 t_2 \\ r_{31} & r_{32} & r_{33} & t_3 \end{bmatrix} \begin{bmatrix} X_p \\ Y_p \\ Z_p \\ 1 \end{bmatrix} \quad (3)$$

From the above two formulas, it can be deduced that the coordinates of the point in space. The coordinate values are

$$\begin{cases} X_p = Z_p x_1 / c_1, \quad Y_p = Z_p y_1 / c_1 \\ Z_p = \frac{c_1 (c_2 t_1 - x_2 t_3)}{x_2 (r_{31} x_1 + r_{32} y_1 + c_1 r_{33}) - c_2 (r_{11} x_1 + r_{12} y_1 + c_1 r_{13})} \end{cases} \quad (4)$$

The above formula is the mathematical expression of the binocular grating measurement model. If the rotation matrix R and the translation matrix T can be known, the image points (x_1, y_1) and (x_2, y_2) of the imaging coordinate system can be calculated by the three-dimensional coordinates of the space point (X_p, Y_p, Z_p) .

3 System Design

3.1 System Structure

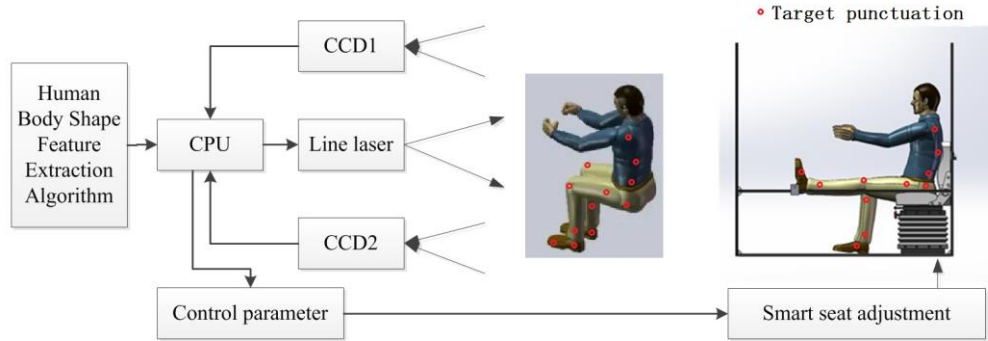


Fig. 2 Intelligent seat adjustment system based on laser 3D scanning

The system was shown in Fig. 2. The processing module controlled the laser 3D scanning equipment to obtain the human body shape features. The laser reflection signal was collected by the CCD and entered the CPU through the data acquisition card. The 3D point cloud filter function was called to filter the input data. Then, through the human body shape feature detection algorithm, the human body shape feature data was extracted and analyzed. In the experiment, the required human feature data mainly referred to the coordinate data of legs and

back, so that two included angle values used to represent comfort. Finally, based on the measurer's leg length, arm length, and waist width, the most comfortable seat position and angle were calculated. Intelligent adjustment of the seat was realized based on the shape characteristics of the human body. During the experiment, when using laser 3D scanning, the target points were used as a marker to obtain the 3D point cloud model of the person and the car seat. Target punctuations were shown in Fig.2.

The test target was a person. He sat in a seat that could be controlled by a circuit feedback system. The research purpose of this paper was to automatically adjust the distance and pitch angle of the seat after sitting on the seat for different purposes, so that the driver can achieve the goal of comfortable driving.

3.1 Control Mode

The mannequin stood on the measuring platform, and the 3D point cloud data was scanned by the laser 3D scanner, which was transmitted to the computer and displayed. The feature points and sections of the human body were automatically extracted from the point cloud with the human body size measurement algorithm, to complete the measurement and display the size.

When a person was sitting in the driving position, the distance between the knee and the car body was different, and this distance had the most comfortable value for a fixed car model. This value can be described by the angle between the lower leg and the thigh. Similarly, the included angle of the seat back also had the most comfortable value, which can be described by the included angle between the thigh and the back. After obtaining the position information of the person with three-dimensional laser, the deviation from the most comfortable value can be calculated, for correcting the position and posture of the seat.

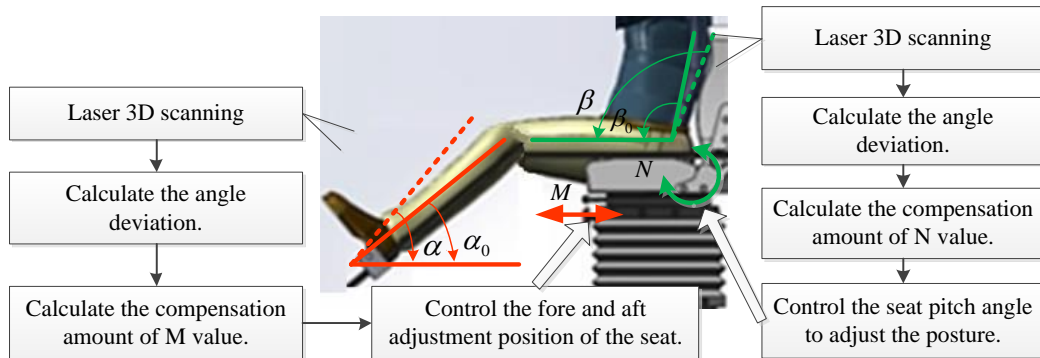


Fig. 3 Diagram of positions and parameters in the control module

As you can see in Fig. 3 above, the seat is used for the driving position of the car, and the adjustment unit is the on-board electronic control module. In the experiment, the position deviation data obtained by laser scanning is imported into

the vehicle electronic control module, and then the seat position and posture can be controlled.

α_0 represents the included angle between the lower leg and the bottom surface at the most comfortable time; α represents the angle between the lower leg and the bottom surface obtained from the actual test. The adjustment degree M of the seat position can be calculated according to the difference between the two values. When $\alpha_0 > \alpha$, the value of M for controlling the forward movement of the seat is decreased. When $\alpha_0 < \alpha$, the value of M for controlling the backward movement of the seat is increased. Finally, when $\alpha_0 = \alpha$, the final control of position adjustment is realized.

β_0 represents the included angle between thigh and waist at the most comfortable time; β represents the angle between the thigh and the waist obtained from the actual test. The adjustment degree N of the seat position can be calculated according to the difference between the two values. When $\beta_0 > \beta$, the value of N for controlling the forward movement of the seat is decreased. When $\beta_0 < \beta$, the value of N for controlling the backward movement of the seat is increased. Finally, when $\beta_0 = \beta$, the final control of position adjustment is realized.

4 Human Body Shape Feature Identify Algorithm

4.1 Determining Feature Points

According to GB/T 23698-2009 "Three-dimensional scanning body measurement method General Requirements" [14], the following feature points should be accurately found for measuring human body size, such as human body center point, cervical vertebra point, nipple point, waist point, knee point, greater trochanter point, most convex point of buttocks, anterior point of left and right armpits, tip of nose point, neck fossa, and so on.

After the approximate location of the feature points is initially determined, the location information of the feature points is accurately extracted. On this basis, according to the position and physiological characteristics of human body feature points, the classification is carried out, and different automatic extraction algorithms have been used respectively. For cervical vertebrae points, nipple points, knee joint points, ankle points, waist points, cervical fossa points and other surface protruding points or joint points, the human body contour analysis method is used to find them. Convert the 3D point cloud data into 2D data for analysis and processing and find the most convex or most concave point in the section. Its feature points can be expressed as

$$P = \left\{ p \in S_i \mid \max(Bv(p_i)), S_i \subset [S_1, S_n] \right\} \quad (5)$$

$Bv(p_i)$ represents the curve of the point p_i on the profile section S_i of the human body surface. It can analyze the depth change of the target position.

The three-dimensional point cloud is layered, and the girth Y is in the approximate area of the feature landmark in the vertical direction. The function can be expressed as

$$L = \{S_i \subset [S_1, S_n] \mid L(S_i) > |L(S_{i+1})\} \quad (6)$$

$L(S_i)$ represents the girth length of the horizontal section.

4.2 Acquisition and recognition of shape point cloud

After the arm length, leg length and other information in the human body shape can be extracted, the calculation of the characteristic data can be completed by the relevant information. The plane calibration plate was used to calibrate the large field of view based on laser 3D scanning system in the test area. A body scanning project was created in the body scanning system software and obtained the 3D point cloud data of the person's shape. The model stands were controlled by the sensor and were set the correction parameters for the specific position of the target. The human body shape feature detection algorithm was used to extract the target in the point cloud and was completed the calculation of length and width. The intelligent seat position was matched by the calculation results and realized the automatic adjustment of the seat by the human body shape characteristics.

According to the core idea of the algorithm and the algorithm flow chart, the specific steps of the algorithm implementation were as follows:

- 1) The point cloud data of the actual position was extracted, and the value of each characteristic point (X_P, Y_P, Z_P) was calculated and solved by equation (4);
- 2) The actual included angles α and β were calculated by connecting the characteristic points. After calculating the leg length of the person to be tested and other information by the characteristic points, the most comfortable included angle values α_0 and β_0 matching with them were selected from the database, to calculate the relationship before the included angle;
- 3) The exact expression of L function was derived from the characteristic parameters;
- 4) The correction functions $M(\alpha, \alpha_0)$ and $N(\beta, \beta_0)$ was imported, and matched (X_P, Y_P, Z_P) with L function, and calculated the correction parameters of seat position and posture;
- 5) After the modified parameters were substituted, the measured value and the optimal value were compared iteratively until they converge to the best value.

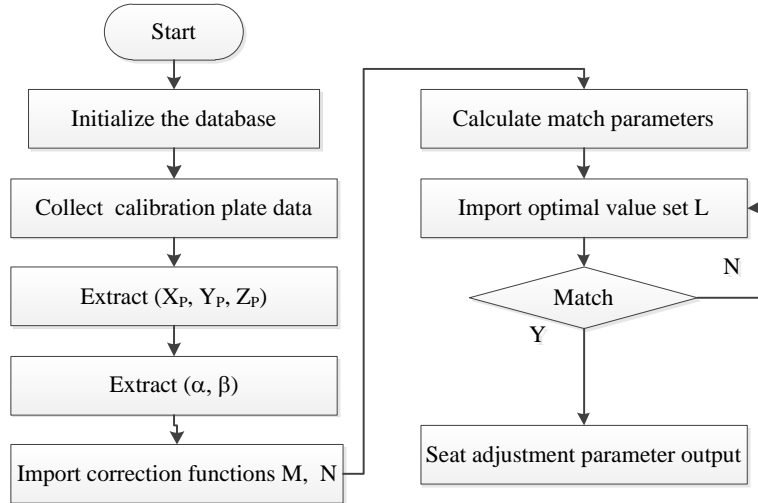


Fig. 4 Flow chart of algorithm program

5 Simulation Analyze

Since the shape features of the human body can be expressed by different surface functions, the data can be obtained by completing the sampling of the surface [14]. The surface can be obtained by extrusion and rotation. The local characteristic curve of the human body generally only contained 1-2 inflection points. The function " $y=-0.2x^2 + \sin(x) + 5x^{-1}$ " was used to sample by MATLAB, and the curve was divided in the interval into 20 equal parts according to the equal-step sampling method. This function contained three inflection points, and the maximum inflection point of the curve from the lower leg to the waist was 3. When the function can be effectively extracted, it showed that the algorithm can effectively extract the features of the local position of the human body. 12 sampling points were added and one sampling point was correspondingly reduced, which achieved the purpose of self-adaptive distribution. In order to highlight the advantages of the control chord height method, the same number of sampling points was selected. Equal step sampling and characteristic location sampling were used in the MATLAB program, as shown in Fig. 5(a).

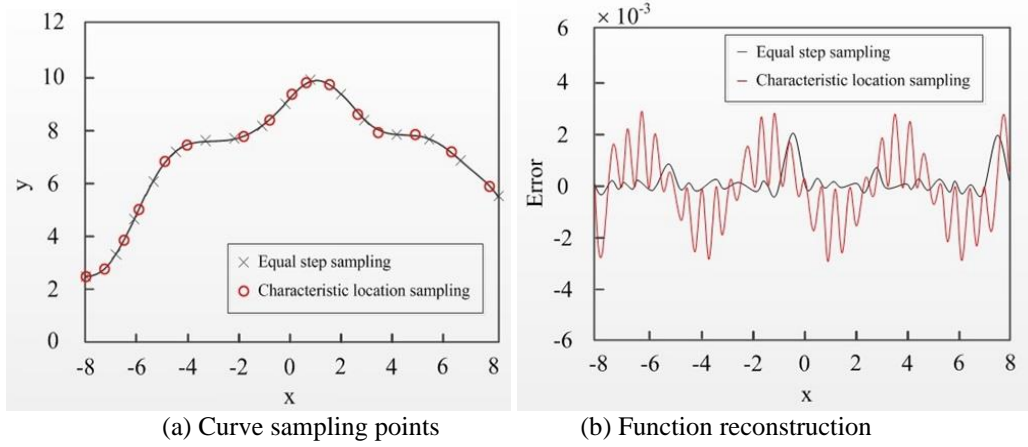


Fig. 5 Parameter change curve

The sampling points obtained by the two methods were fitted with known curve functions respectively, as shown in Fig. 5(b). The figure showed that the deviation between the control chord height method and the known curve function was smaller, and the overall curve change trend was gentler. It showed that the control chord height method can be better to solve the problem of uneven surface curvature. For characteristic location sampling, the error envelope was closer to a sine wave signal. It showed that the use of characteristic location sampling had a positive effect on improving the accuracy of signal inversion.

6 Experiments

The VW416 driver's seat (Type: HL02WJ, 30G 881 021N) for the Volkswagen Lanjing 2022 330TSI was selected for the experiment, and the 5WA 959 760H electronic control module was used for automatic position adjustment control of the seat. The target point on the driver was acquired by ATOS optical 3D scanner. The wavelength range of laser was 400-500nm, the camera position was 300mm, and the test volume was 300mm * 200mm * 200mm.

6.1 Accuracy Test

In order to verify the accuracy and stability of the photogrammetry-based camera calibration method, the calibration of the system was performed using a calibration plate. The results of 16 calibrations were shown in Fig. 6.

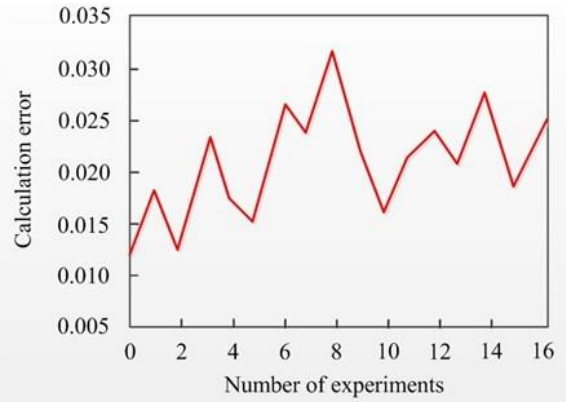


Fig.6 Resource computed supply curve

The results of the 15 system calibration errors were shown as fig.6. The minimum of pixels was of 0.016, and the maximum of pixels were 0.046, and the average of pixels was 0.034. The errors were all better than 0.05 pixels, which indicated that the system calibration error. It can be realized by the camera calibration method based on photogrammetry. The fluctuation range of the calibration results was very small, indicating calibration method.

The experiment's purpose was to verify the effect of digital image correlation matching techniques based on seed points and binocular stereo vision reconstruction. Following the experimental steps in Section 2.1, we conducted three sets of human scanning experiments. The three sets of point clouds were shown in Fig. 6, the scanning time was all within 0.1s. It reduced the error caused by human body shake, and it improved the user experience of the XTBodyScan system [15]. It was the complete human point cloud model reconstructed by seed point-based image matching technology. The scans did not show significant differences for models of different heights and weights. Therefore, this method had a certain robustness.

6.2 Surface Shape Feature Measurement

The surface of the human body shape was extracted. According to the characteristics of the curve function and the proposed adaptive measurement point distribution method, the appropriate sampling points were selected. Finally, the robot was controlled to use the sampling points as the measurement station to complete the shape measurement. The robot TCP [16] pose coordinate information during the measurement process was shown in Table 1.

Table 1

Human body shape surface scan path pose						
Points	Rx(°)	Ry(°)	Rz(°)	X(mm)	Y(mm)	Z(mm)
1	11.5382	-46.4818	35.6248	244.264	-39.124	542.152
2	59.6871	-58.8268	15.3694	228.478	-215.261	154.487

3	92.2158	-18.9331	75.3265	251.158	-541.847	214.369
4	99.1474	-82.6745	84.2519	253.658	368.814	-548.965
5	11.2611	-22.2257	56.3264	241.415	218.933	-51.244
6	150.5752	-34.1648	81.3624	225.258	282.674	674.168
7	80.0025	-25.1427	55.3264	231.365	522.225	571.265
8	156.5847	-18.5916	77.3655	247.548	121.145	615.358
9	114.2684	-50.7157	88.3658	244.125	129.884	63.524
10	99.2568	-48.3669	24.3658	284.244	253.248	84.369

7. Conclusions

Aiming at intelligent adjustment of the seat, automatic human body shape scanning system was proposed. It obtained the human body shape point cloud through 3D laser scanning and completed the feature location extraction with the human body shape feature recognition algorithm. It verified the feasibility of the system by simulation analysis and experimental test. It had certain advantages by the acquisition of human body shape and the adjustment of intelligent vehicle seat. However, it needs to be further improved the total amount of point cloud data, for increasing the processing speed of the system, and it's also the main research expectation in the next step of this paper.

Acknowledgements

This work was supported by the Changchun Science and Technology Project, Jilin Province, China (Grant No. 21ZY55), the Science and Technology Development Program of Jilin Province, China (Grant No. 20210201053GX).

R E F E R E N C E S

- [1] Sun Mi, Park, Yun, et al. The Verification of Accuracy of 3D body scan data-focused on the cyberware WB4 Whole body scanner, Journal of the Korea Fashion & Costume Design Association, 2012, volume 14(1): 81-96.
- [2] Michael Z, Martinek M, Greinerg, et al. Automatic reconstruction of personalized avatars from 3D face scans, Computer Animation and Virtual Worlds, 2011, volume 2(3), 195-202.
- [3] Henry P, Krainin M, Herbste, et al. RGB-D mapping: using Kinect-style depth cameras for dense 3D Modeling of indoor environments, The International Journal of Robotics Research, 2012, volume 31(5): 647-663.
- [4] Richard A, Izadis, Hilliges O, et al. Kinect fusion: real-time dense surface mapping and tracking, 2011 IEEE International Symposium on Mixed and Augmented Reality, Basel: IEEE, 2011.
- [5] Charlie Cl, Wang, Yu Wang, et al. Virtual human Modeling from photographs for garden industry, Computer-Aided Design, 2003, volume 35(6): 577-589.
- [6] Chen Jiayu, Zhong Yueqi, Yu Zhicai. 3D human Body model reconstruction based on binary image, Wool Textile Journal, 2020, volume 48(9): 61-67.
- [7] Wu Xucheng. Modeling and motion simulation method of Virtual main tenance human body based on Unity3D, Science and Technology Horizon, 2019, volume3 (11): 50-51.

- [8] Wang Meiliang, SHEN Yang. The 3D human body modeling for virtual fitting based on the key Characteristic parameters, Heidelberg: Transactions Edutainment XIV, 2018.
- [9] Liu Yongmei, LI Rong, XIAO Ping. Research on the construction of series virtual human platform based on Children's body shape standard, Shangong Textile Economy, 2020, volume 2(8): 5-9.
- [10] Yeong H K, Sungmin K. Develop ment of bulletproof pad design system using 3D body scan data, International Journal of Clothing Science and Technology, 2019, volume 31(6): 456-638.
- [11] Danckaers F, Huysmans T, Hallemans A, et al. Posture normalization of 3D body scans, Ergonomics, 2019, volume 62(6): 834-848.
- [12] Chu Ch, Tsai Y T, Kwok C, et al. External-based statistic model for semantic parametric design of human body, Computers in Industry, 2010, volume 61(6): 541-549.
- [13] Hilton A, Bersford D, Gentils T, et al. Whole-body modelling of people from multiview images to Populate virtual worlds, Visual Computer, 2000, volume 16(7):411-436.
- [14] Clarkson S, Wheat J, Heller B, et al. Assessing the suitability of the Microsoft Kinect for calculating person specific body segment parameters, Computer Vision-ECCV 2014 Workshops, 2014: 372-385.
- [15] Rodríguez J C, Sergiyenko O Y, Preciado L C B, et al. Optical monitoring of scoliosis by 3D medical laser scanner, Optics and Lasers in Engineering, 2014, volume 54(1): 175-186.
- [16] Xu B G, Freeland J H, Pepper M R, et al. Evaluation of adult body adiposity, size, and shape by stereovision imaging, Journal of Testing and Evaluation, 2012, volume 41(1): 1-10.